FERMILAB
SEP 29 1999
LIBRARY

Institute of Theoretical and Experimental Physics

1-99

A. Asratyan, G. Davidenko, A. Dolgolenko,
V. Kaftanov, M. Kubantsev, V. Verebryusov

ITEP 1-99

A Detector for Probing the $\nu_\mu' \to \nu_\tau$ Transition over Short and Medium Baselines

Fermilab Library
0 1160 0070486 0

Moscow 1999

UDK 539.1 M-16

A DETECTOR FOR PROBING THE $\nu_\mu \to \nu_\tau$ TRANSITION OVER SHORT AND MEDIUM BASELINES: Preprint ITEP 1-99/

A.Asratyan, G.Davidenko, A.Dolgolenko, V.Kaftanov, M.Kubantsev, V.Verebryusov - M ., 1999 - 24p.

A detector scheme is proposed for studying the $\nu_\mu \to \nu_\tau$ transition over medium and short baselines in appearance mode. A distributed target is formed by layers of low-Z material, emulsion-plastic-emulsion sheets, and air gaps in which τ decays are detected. Target modules are alternated by drift chambers that provide electronic tracking. The tracks of charged secondaries, including electrons, are momentum-analyzed by curvature in magnetic field using hits in successive thin layers of emulsion. The electronic and three-prong decays of the τ will be efficiently detected in addition to the muonic and semihadronic one-prong modes. At a medium-baseline location on mount Jura in the existing neutrino beam of CERN-SPS, the detector will show good sensitivity to a $\nu_\mu \to \nu_\tau$ transition driven by a mass difference of $\Delta m^2 \sim 1$ eV^2.

Fig. - 9, ref. - 17.

© Институт теоретической экспериментальной физики , 1999

1 Introduction

Transitions between the neutrinos of different flavors are vigorously pursued using the solar, atmospheric, reactor, and accelerator neutrinos. An accelerator experiment using neutrinos from π^+ and μ^+ decays at rest over an effective baseline of $L/E \sim 1$ m/MeV, LSND at Los Alamos [1], has reported a positive signal in the channel $\bar{\nu}_\mu \to \bar{\nu}_e$ with a probability of $\sim 3 \times 10^{-3}$. The upper limits of other accelerator and reactor experiments [2, 3] suggest that the $\bar{\nu}_\mu \to \bar{\nu}_e$ oscillation is driven by a mass difference squared, Δm^2, between some 0.3 and 2.3 eV^2. As the observed deficit of muon neutrinos from the atmosphere is claimed to be driven by a much smaller mass difference of some 10^{-3} eV^2 [4], this may qualify as a bigger Δm^2 of the two required by a general scheme of transitions among three Dirac neutrinos.

Qualitatively, there are sound reasons to believe that the transition driven by the bigger Δm^2 must primarily manifest itself in the $\nu_\mu \to \nu_\tau$ channel. First, one may expect that the mass hierarchy of neutrinos follows that of corresponding charged leptons, so that ν_τ should be the most massive. On the other hand, the analogy with the known pattern of quark mixings suggests that mixings between the neighboring neutrino flavors (*i.e.*, ν_e–ν_μ and ν_μ–ν_τ) should be the strongest, while that for ν_e–ν_τ may be substantially weaker.

Thereby, one is encouraged to search for the $\nu_\mu \to \nu_\tau$ transition in the Δm^2 region of 0.3–2.3 eV^2, where the existing restrictions on its probability

are not compelling [5, 6]. This "high-frequency" $\nu_\mu \to \nu_\tau$ transition can be best investigated over an effective baseline of $L/E \sim 1$ km/GeV (to probe the Δm^2 values around 1 eV^2) in a ν_μ beam with mean energy well above the threshold for τ production (to detect the ν_τ in the appearance mode). Both conditions are ideally met by using the existing wide-band ν_μ beam of the CERN-SPS accelerator ($\langle E_\nu \rangle = 27$ GeV by flux) for irradiating a detector deployed in a "medium-baseline" location of Mount Jura at some 17 km from the ν_μ source [7].

In this paper, we propose a conceptual scheme of a detector aimed at probing this "high-frequency" $\nu_\mu \to \nu_\tau$ transition over the medium and short baselines, that employs the technique of nuclear emulsion [6, 8]. Like the planned experiment OPERA [9], we rely on the principle of ECC: layers of thin emulsion are only used as a tracker for events occurring in passive material. But unlike OPERA, we aim at constructing a distributed target with low density and large radiation length [10], so that either muons, hadrons, and electrons can be momentum-analyzed by curvature inside the target itself. Accordingly, the target largely consists of low-Z material like carbon in a form of carbon-fiber composite. Apart from narrow gaps instrumented with drift chambers that provide an electronic "blueprint" of the event, the target is built as a compact homogeneous volume in ambient magnetic field. Owing to relatively weak multiple scattering in low-Z material, the successive layers of thin emulsion may act as an "emulsion spectrometer" in analyzing the momenta of charged secondaries and conversion electrons. In untangling the topologies of neutrino events, the detector will operate very much like a bubble chamber.

2 The detector

The detector is primarily designed for the Jura site [7] in the existing ν_μ beam of CERN-SPS [8, 10], that provides an effective baseline of $L/E \sim 1$ km/GeV

for the $\nu_\mu \to \nu_\tau$ transition. A very similar apparatus can also be deployed on the "near" site (at 1850 m from the proton target) in the proposed ν_μ beam pointing from CERN to Gran Sasso [11], where $L/E \leq 0.1$ km/GeV. Yet another possibility is a new short-baseline experiment in the existing beam of CERN-SPS, see [12].

The ECC-like fine structure of the detector is depicted in Fig. 1. The 6-mm-thick basic element comprises a 1-mm-thick plate of passive material (960 μm of carbon plus 40 μm of copper), an emulsion-plastic-emulsion sheet (50 + 100 + 50 μm), and an air gap in which τ decays are selected (4800 μm). The successive elements form a stack with a mean density of $\rho = 0.49$ g/cm^3 and with an effective radiation length of $X_0 = 52.6$ cm. (These values of ρ and X_0 are very similar to those of bubble chambers with neon-hydrogen filling.) Note that the element does not feature the second emulsion-plastic-emulsion sheet (ES) downstream of the gap: the idea is to detect the kink using track segments in the ES's of two successive elements. As soon as the fitted position of the kink lies within the passive plate of the next element, the candidate event must be dropped.

By adding a thin layer of copper downstream of carbon, we slightly compromise the radiation length but effectively increase the fraction of τ's that decay in the air gap rather than in passive material. That the proportion of copper events is increased by the geometric effect is illustrated by Fig. 2. Of all τ's produced in the passive plate, some 51% are seen to have decayed in the downstream gap.

On the technical side, a 40-μm-thick copper foil can be glued to the 960-μm-thick plate of carbon-fiber composite. Carbon composite can be molded in brush-like form, with rigid 5-mm "bristles" on one side supporting the ES of the upstream element and creating the necessary drift distance. (This is only possible because we have just one ES per element.) The positions of the thin bristles will be tabulated, and secondary vertices that match these positions will be dropped. Thus, all we have in the gap is plain air, so that the

three-prong decays of the τ are no longer overshadowed by pion reinteractions in the honeycomb [9].

The target as a whole, as shown in Fig. 3 for a medium-baseline option, has a transverse area of 250×250 cm^2 and consists of 900 elements grouped in 30 modules of $0.34X_0$ thickness. The gap between adjacent modules is 4 cm, and is instrumented by a multisampling drift chamber with an area of 300×300 cm^2. On total, the target contains 14.3 tons of passive material and 2.1 tons of standard emulsion (or a lesser amount of diluted emulsion [9], that may be warranted by a relatively low occupancy at a medium-baseline location). The 6.6-m-long target can be deployed inside the existing magnet of the NOMAD detector [10], that has a magnetic volume of $3.5 \times 3.5 \times 7.5$ m^3 and delivers a field of up to 0.7 Tesla. For the short-baseline location, the transverse area of the module is decreased to 180×180 cm^2, thus reducing the total amounts of passive material and of emulsion to 7.4 and 1.1 tons, respectively.

The scheme also features an electromagnetic calorimeter (EMCal) of fine-grained lead glass, that has circular shape with 3.5-m diameter. This is aimed at identifying electrons from the downstream modules and at detecting those photons that failed to convert in the target. The 4.5-m gap between the target and the EMCal is also instrumented by drift chambers. The design of the muon system is not discussed in this paper.

3 Event reconstruction

The mean energy of ν_τ-induced CC collisions is over 50 GeV, and therefore the bulk of τ events will feature several energetic charged particles of either sign. Using the drift-chamber image of the event, we will be able to reconstruct and momentum-analyze their tracks and, at the very least, find the 30-layer-thick module in which the collision occurred.

In a medium-baseline experiment, the occupancy of ESs will be relatively low, so that we can scan back along a fitted track, starting from the downstream ES of this module. As soon as the layer of origin is reached, a few successive ESs of the nearby elements must be fully scanned over relatively small areas towards finding the stubs of all other tracks associated with the primary vertex. To refine the alignment of the ESs, a sufficient number of long tracks of energetic muons must be fully reconstructed in emulsion. This first stage of emulsion scanning will yield a relatively small number of events featuring decay signatures (either a kink or a trident in the air gap just downstream of primary vertex). For the candidate events only, the second stage will be to scan down all tracks from the primary vertex and to find and measure the conversions of secondary photons in the target.

As soon as a track is found in ESs, the estimate of its momentum can be refined using hits in emulsion (this primarily applies to electrons). That the successive ESs may act as an "emulsion spectrometer" is due to relatively weak multiple scattering in carbon. As in a bubble chamber, an electron is identified by change of curvature and by emission of brems.

For the short-baseline option, a much higher occupancy of ESs may dictate a general scan of the relatively small amount of emulsion (1.1 tons). This may be allowed by the rapidly evolving technique of automatic scanning [13, 9]. Then, track stubs in the ESs can be put together using the drift-chamber "blueprint" of the event. The general scan of all emulsion can be avoided, if the system of drift chambers is augmented by large planes of silicon detectors [14]. A silicon plane (that provides a single XY measurement) after every two or three modules may be enough, as scanback can be done along a stiff track that has already been reconstructed on electronic level.

Detector responses to various decays of the τ are investigated through a GEANT-based simulation, as described below. We also estimate the null-limit sensitivity of the proposed experiment to the $\nu_\mu \rightarrow \nu_\tau$ transition.

4 Simulation procedure and assumptions

For the τ's emitted in either the deep-inelastic and quasielastic $\nu_\tau N$ collisions, we generate the two leptonic decays and three semileptonic (quasi-)two-body decays: $\tau^- \to \pi^-\nu$, $\tau^- \to \pi^-\pi^0\nu$ that is mediated by the resonance $\rho^- \to \pi^-\pi^0$, and $\tau^- \to \pi^-\pi^+\pi^-\nu$ that is mediated by the resonance $a_1^- \to \pi^-\pi^+\pi^-$. Polarization of the τ, that affects the angular distribution of decay products in the τ frame, is accounted for. The lineshapes of intermediate resonances are generated in Gaussian forms.

Thus generated τ events are then propagated through the detector using GEANT. In fitting a track, we assume that each tracker traversed (either a ES or a drift chamber) provides two spatial points, that are then smeared by spatial resolutions (2 and 150 μm, respectively). Then, particle momentum is obtained by fitting the "smeared" trajectory in uniform magnetic field of 0.7 Tesla. Likewise, the EMCal resolutions in the position of the hit and in deposited energy are approximated as $\delta x = \delta y = 2$ mm and δE (GeV) $= 0.05\sqrt{E} + 0.02E$, respectively.

For the τ decay to be detectable on apparatus level, we assume that the following minimum conditions must be satisfied:

- the τ must have decayed in the drift gap;
- all charged daughters of the τ must be momentum-analyzed by curvature and reliably sign-selected;
- for a one-prong decay to a charged daughter d (either a muon, electron, or pion), the kink angle must be suffiently large: $\theta_{\tau d} > 20$ mrad;
- for all decays including $\tau^- \to \pi^-\pi^+\pi^-\nu$, the momentum of either charged daughter must exceed 1 GeV, and its emission angle must lie within 400 mrad of beam direction;
- the track of any charged daughter of the τ must fire at least one drift

chamber.

These "minimum selections" are implicitly included in all distributions for τ events in the detector, as illustrated below. The adopted condition of normalization is that, for a given decay channel of the τ, unity corresponds to the total number of primary vertices in passive material prior to any selections.

5 Detecting the leptonic decays of the τ

Of the τ's decaying through either of the two leptonic channels, $\tau^- \to \mu^-\nu\bar{\nu}$ and $\tau^- \to e^-\nu\bar{\nu}$, some 43% survive the aforementioned minimum selections. As electrons often generate showers in thick emulsion, in experiments like E531 [6] and CHORUS [8] the electronic decays of the τ are detected much less efficiently than the muonic ones. One of the major goals of the proposed experiment is to detect the decay $\tau^- \to e^-\nu\bar{\nu}$ almost as efficiently as $\tau^- \to \mu^-\nu\bar{\nu}$.

In fitting the e^- track in magnetic field, one must take into account the variation of curvature due to energy loss in successive layers of the target. Actually fitted is the restricted segment of the e^- track over which the actual loss of energy does not exceed 20% (so that the e^- energy at endpoint always exceeds 800 MeV). This segment is required to include no less than 5 trackers (either ES's or drift chambers). For thus selected segments of the e^- tracks, the length in z is plotted in Fig. 4.

We compute an "ideal trajectory" for a given value of electron momentum p_e, to which the observed trajectory is then fitted, using GEANT. In doing so, we switch off multiple scattering and radiation losses, but instead reduce the momentum "by hand" in each layer of the target by the same amount Δp that is treated as an empirical parameter. The value of Δp is selected so as to obtain (i) an unbiased estimate of electron momentum ($\langle p_e^{\rm meas}/p_e^{\rm true}\rangle \sim 1$) and (ii) a reasonable value of χ^2. Due to multiple scatter-

ing, the fit is but marginally sensitive to increasing the spatial error in the ES from 2 up to 10 μm.

Dropping the poorly fitted electrons with $\chi^2/NDF > 3$, we then plot the ratio between the fitted and true momenta, $p_e^{\rm meas}/p_e^{\rm true}$, in Fig. 5. The same ratio is then separately plotted for two regions of electron momentum: $p_e < 5$ GeV and $p_e > 5$ GeV. Of the $\tau^- \to e^-\nu\bar{\nu}$ decays of all τ's produced in passive plates, nearly 38% are seen to be "good" events that survive the minimum selections (see above) and feature an electron that can be reliably detected and sign-selected (that is, $\delta p_e/p_e < 0.35$). On average, the e^- momentum is measured to a precision of some 13%.

We may conclude that the proposed detector will indeed select the electronic decays of the τ almost as efficiently as the muonic ones. A comparison between the two leptonic modes will provide an important handle on the self-consistency of an observed $\nu_\mu \to \nu_\tau$ signal.

6 Reconstructing the (quasi-)two-body decays of the τ

An experiment aimed at the $\nu_\mu \to \nu_\tau$ transition should be capable of convincingly interpreting and demonstrating even a relatively small τ signal. For this, an appreciable fraction of the signal must be unambiguously reconstructed as τ decays rather than the decays of anticharm. Such distinctive signatures can only be provided by the (quasi-)two-body semileptonic decays of the τ: $\tau^- \to \pi^-\nu$, $\tau^- \to \rho^-\nu$, and $\tau^- \to a_1^-\nu$.

In a (quasi-)two-body decay $\tau^- \to h^-\nu$, "transverse mass" is defined as $M_{\rm T} = \sqrt{m_h^2 + p_{\rm T}^2} + p_{\rm T}$, where m_h and $p_{\rm T}$ are the h^- mass and transverse momentum with respect to τ direction. The two-body kinematics dictate that the $M_{\rm T}$ distribution should reveal a very distinctive peak just below $M_{\rm T}^{\rm max} = m_\tau$, see Fig. 6. This "Jacobian cusp", that may provide a characteristic signature of the τ, rapidly degrades with increasing $\Delta p/p$ for the decay

products. Needless to say, analyzing the $\tau^- \to \pi^-\pi^0\nu$ decays also requires good reconstruction of $\pi^0 \to \gamma\gamma$ decays in the detector. The $M_{\rm T}$ technique for identifying massive parents by two-body decays in emulsion was proven by observing the relatively rare decays $D_s^+(1968) \to \mu^+\nu$ against a heavy background from other decays of charm [15].

The momentum resolution for the π^- from the decay $\tau^- \to \pi^-\nu$, as illustrated in Fig. 7, on average amounts to some 7%. The smeared and unsmeared values of $M_{\rm T}$ for the decays $\tau^- \to \pi^-\nu$ and $\tau^- \to \pi^-\pi^+\pi^-\nu$, that involve only charged pions, are plotted in Fig. 6. The Jacobian cusps of the original $M_{\rm T}$ distributions for these decay channels are not destroyed by apparatus smearings of the proposed detector. The minimum selections are seen to accept some 40% of all $\tau^- \to \pi^-\nu$ decays and 27% of all $\tau^- \to \pi^-\pi^+\pi^-\nu$ decays.

In order to select the decays $\tau^- \to \pi^-\pi^0\nu$, one has to reconstruct the π^0 from photon conversions that may occur either in the target or in the EMCal. In estimating the energy of a photon that has converted in the target, we count only those conversion electrons that have fired at least one drift chamber (these are then momentum-analyzed by curvature). The measured invariant mass of two detected photons, as plotted in Fig. 8, shows a distinct π^0 signal. Selecting the π^0 in a mass interval of 115–155 MeV, we then plot the measured value of $M_{\rm T}$ for the decay $\tau^- \to \pi^-\pi^0\nu$, see Fig. 6. Again, the Jacobian cusp of the original $M_{\rm T}$ distribution persists in the smeared distribution. Of the $\tau^- \to \pi^-\pi^0\nu$ decays of all τ's produced in passive material, some 10% are seen to survive the minimum selections for the π^- and the above selections for the π^0.

7 Sensitivity to neutrino oscillations

In the proposed experiment, the τ's will be detected through essentially all decay modes, including the two leptonic channels and either the one-prong

and three-prong semihadronic channels. For those τ decay channels that have actually been simulated in the detector, the estimated fractions of all decays that survive the minimum selections, or detection efficiencies, are listed in Table 1. (Note that here we do not require the π^0 from $\tau^- \to \pi^-\pi^0\nu$ to be reconstructed.)

Towards removing the background from the decays of strange particles, the one-prong decays of the τ must be further selected in p_T of the charged daughter with respect to τ direction: $p_T > 250$ MeV. The resulting acceptances are also quoted in Table 1 for the modes $\tau^- \to \mu^-\nu\bar{\nu}$, $e^-\nu\bar{\nu}$, $\pi^-\nu$, $\pi^-\pi^0\nu$, and $\pi^-\pi^+\pi^-\nu$. For these decay channels of the τ, the acceptance-weighted branching fractions add up to some 0.28. Roughly accounting for the other one-prong and three-prong channels, we estimate that nearly 32% of all produced τ's will be accepted.

Decay channel	Branching fraction	Detection efficiency	Acceptance with $p_T > 250$ MeV for one-prongs	Acceptance times branching
$\tau^- \to \mu^-\nu\bar{\nu}$	0.174	0.43	0.40	0.070
$\tau^- \to e^-\nu\bar{\nu}$	0.178	0.38	0.36	0.064
$\tau^- \to \pi^-\nu$	0.113	0.40	0.40	0.045
$\tau^- \to \pi^-\pi^0\nu$	0.252	0.38	0.30	0.076
$\tau^- \to \pi^-\pi^+\pi^-\nu$	0.094	0.27	0.27	0.025

Table 1: The branching fractions, detection efficiencies, and acceptances (the latter including $p_T > 250$ MeV for the one-prong modes) for those decay channels of the τ that have been simulated in the detector.

In a short-baseline experiment that will collect millions of neutrino events, an important source of background to the τ signal is anticharm production in those antineutrino-induced CC events in which the primary μ^+ has been misidentified in the detector. That the τ, unlike anticharm, is emitted back-to-back with primary hadrons in the transverse plane allows to sup-

press the anticharm background by additional kinematic cuts (see, *e.g.*, the proposals [12, 16]). For our crude estimate of the null-limit sensitivity for the short-baseline option, these additional selections are assumed to accept some 50% of the τ signal, while suppressing the anticharm background to a negligible level.

At the medium-baseline location on mount Jura, the rate of ν_μ-induced CC collisions has been estimated in [17] as 843 events per ton of target per 10^{19} protons delivered by CERN-SPS. Assuming 10^{20} delivered protons which corresponds to 3–4 years of operation, the proposed detector will collect nearly 1.2×10^5 CC events. Even if the probability of the $\nu_\mu \to \nu_\tau$ transition is as small as 0.3% [1], we will detect some 58 τ events with a negligibly small background from the decays of strange and anticharm particles. Alternatively, a zero signal will translate into the 90% exclusion plot of Fig. 9. Also shown is the null-limit exclusion plot for the proposed short-baseline experiment in the NGS beam [11].

Also note that the proposed detector will very efficiently identify, momentum-analyze, and sign-select the primary electrons from CC collisions of the electron neutrinos and antineutrinos. The energy of incident ν_e ($\bar{\nu}_e$) will be estimated to better than 10%. If at the Jura site the transition $\nu_\mu \to \nu_e$ indeed occurs with a probability of some 0.003 as in LSND [1], in an exposure of 10^{20} protons on target we will detect and reconstruct some 290 $\nu_e N \to e^- X$ events due to oscillated neutrinos against a background of nearly 540 CC events due to the original ν_e component of the beam [17]. As the original ν_e component of the beam is substantially harder than the ν_μ component, a $\nu_\mu \to \nu_e$ signal will effectively reduce the mean energy of $\nu_e N \to e^- X$ events. By comparing the observed value of $\langle E_{\nu_e} \rangle$ with the prediction for the original ν_e component, one may probe the mass difference that drives the $\nu_\mu \to \nu_e$ oscillation.

8 Summary

A conceptual detector scheme is proposed for studying the $\nu_\mu \to \nu_\tau$ transition over the medium and short baselines. A distributed target is formed by layers of low-Z material, emulsion-plastic-emulsion sheets, and air gaps in which τ decays are detected. Target modules with mean density of 0.49 g/cm^3 and radiation length of 52.6 cm, that are similar to those of a bubble chamber with neon-hydrogen filling, are alternated by drift chambers that provide electronic tracking of neutrino events. The tracks of charged secondaries, including electrons, are momentum-analyzed by curvature in magnetic field using hits in successive thin layers of emulsion and in drift chambers. Electrons are identified by change of curvature and by emission of brems. Those photons that failed to convert in the target are detected by an electromagnetic calorimeter based on Cherenkov lead glass, that also helps identify the electrons from a few downstream modules of the target. Apart from the muonic and semihadronic one-prong modes, the electronic and three-prong decays of the τ will be efficiently detected. At a medium-baseline location on mount Jura in the existing neutrino beam of CERN-SPS, the detector will be sensitive to either the $\nu_\mu \to \nu_\tau$ and $\nu_\mu \to \nu_e$ transitions driven by a mass difference of $\Delta m^2 \sim 1$ eV^2.

This work was supported in part by the CRDF foundation (grant RP2-127) and by the Russian Foundation for Fundamental Research (grant 98-02-17108).

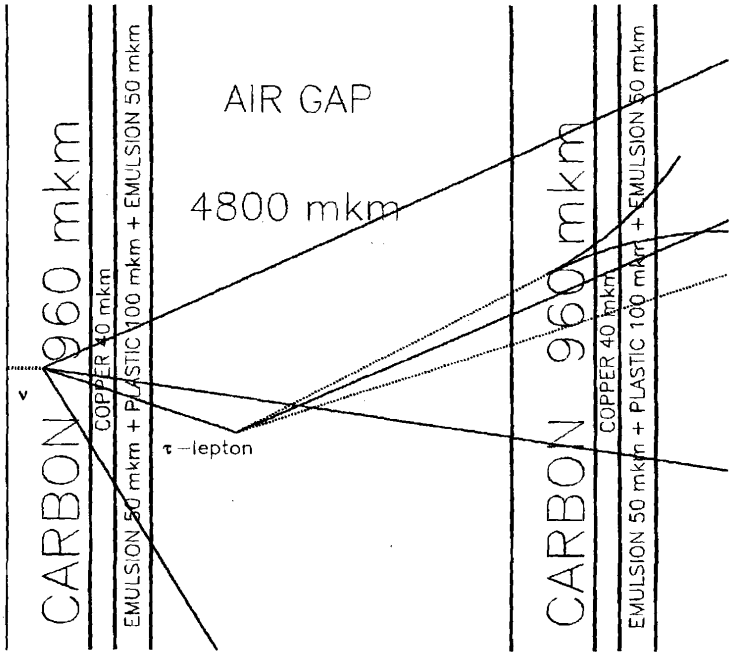

Figure 1. Schematic of the fine structure of the target, showing the carbon–copper plates (960 + 40 μm), emulsion-plastic-emulsion sheets (50 + 100 + 50 μm), and air gaps in which τ decays are selected (4800 μm).

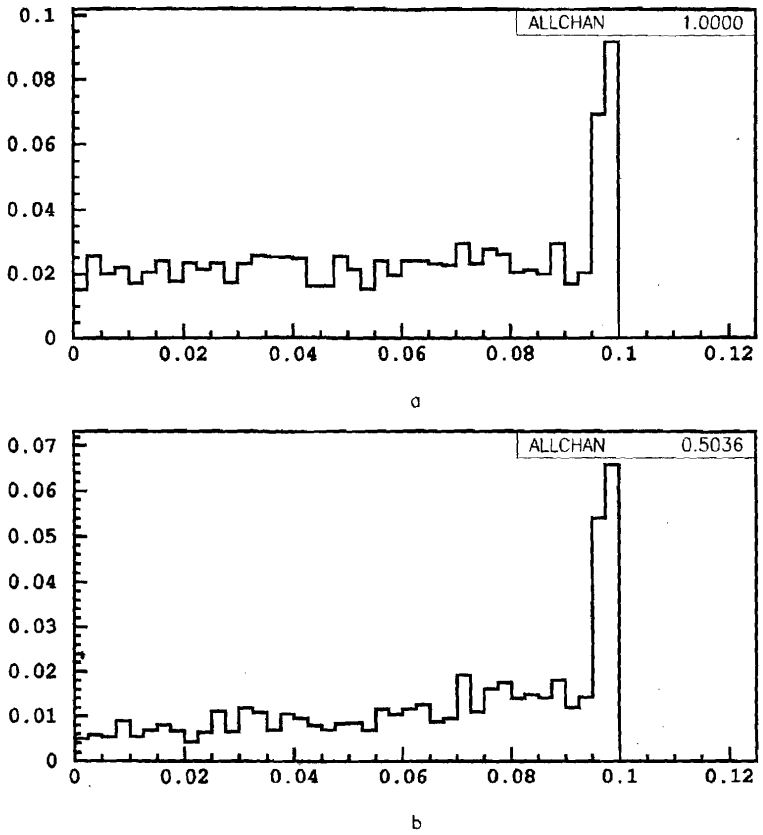

Figure 2. The z-distribution of primary vertices through the carbon–copper plate for all events (a) and for those events in which the τ has decayed in the drift gap (b). Of all τ's produced in passive material, some 51% have decayed in the downstream gap.

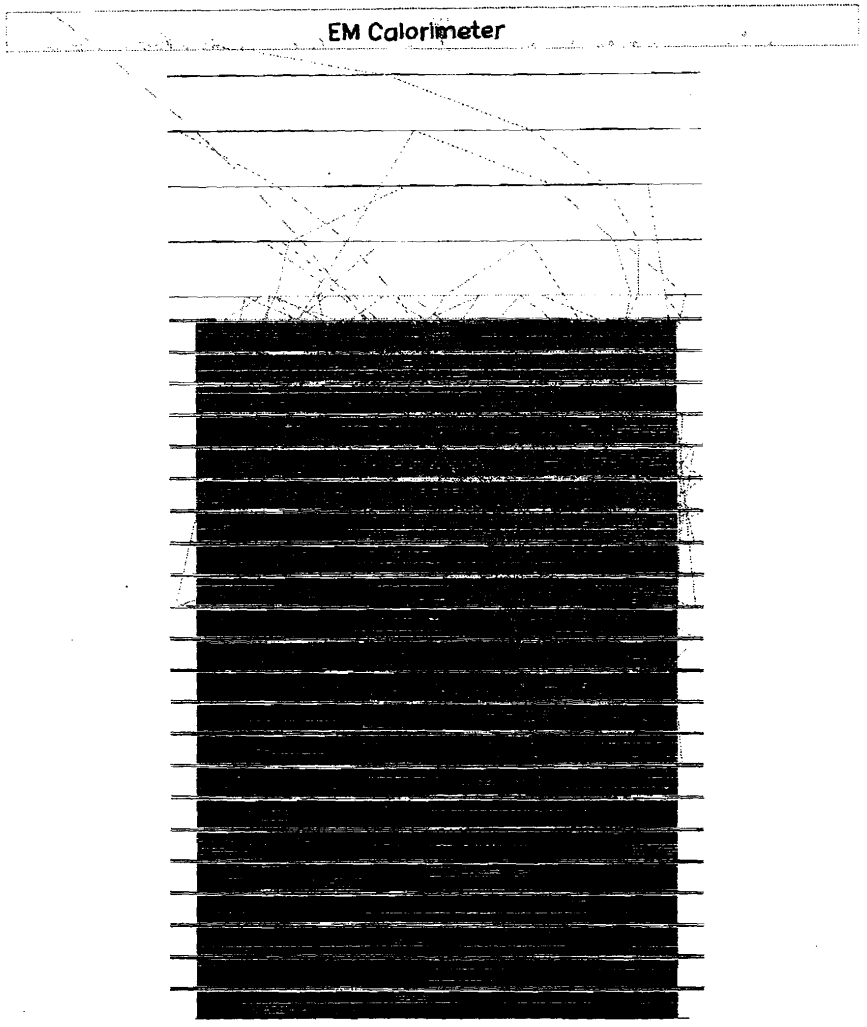

Figure 3. The scheme of the detector for a medium-baseline location, showing the target modules, the drift chambers, and the electromagnetic calorimeter. On total, the target comprises 14.3 tons of passive material (carbon and copper) and 2.1 tons of (standard) emulsion. The magnet is not shown. Overlaid is a typical $\tau^- \to \pi^-\pi^0\nu$ event in which the primary hadrons have been suppressed for clarity.

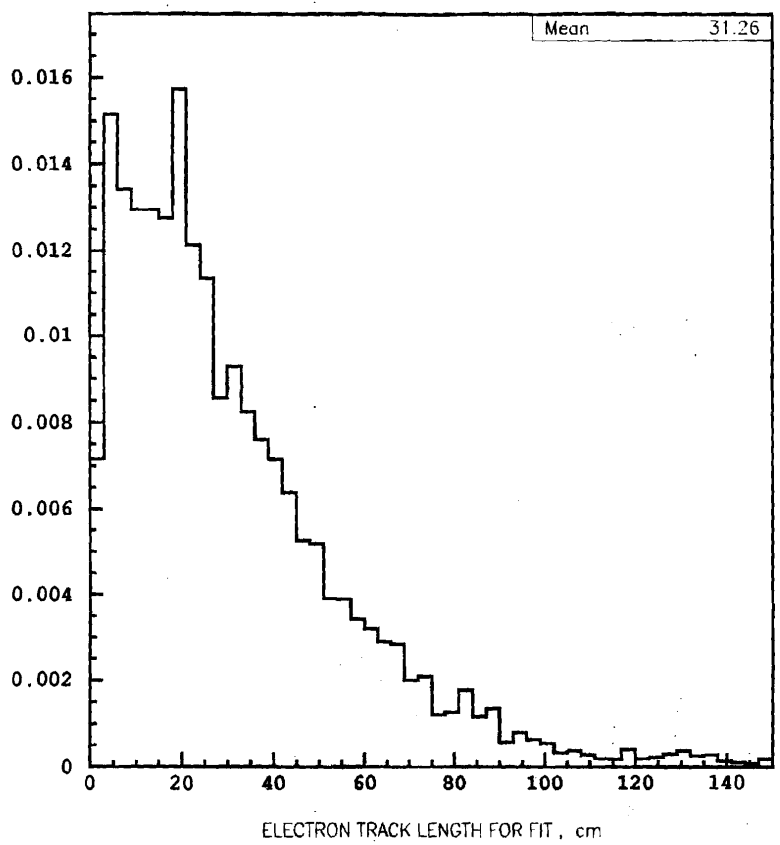

Figure 4. Length in z of the track segment used for analyzing the e^- momentum by curvature.

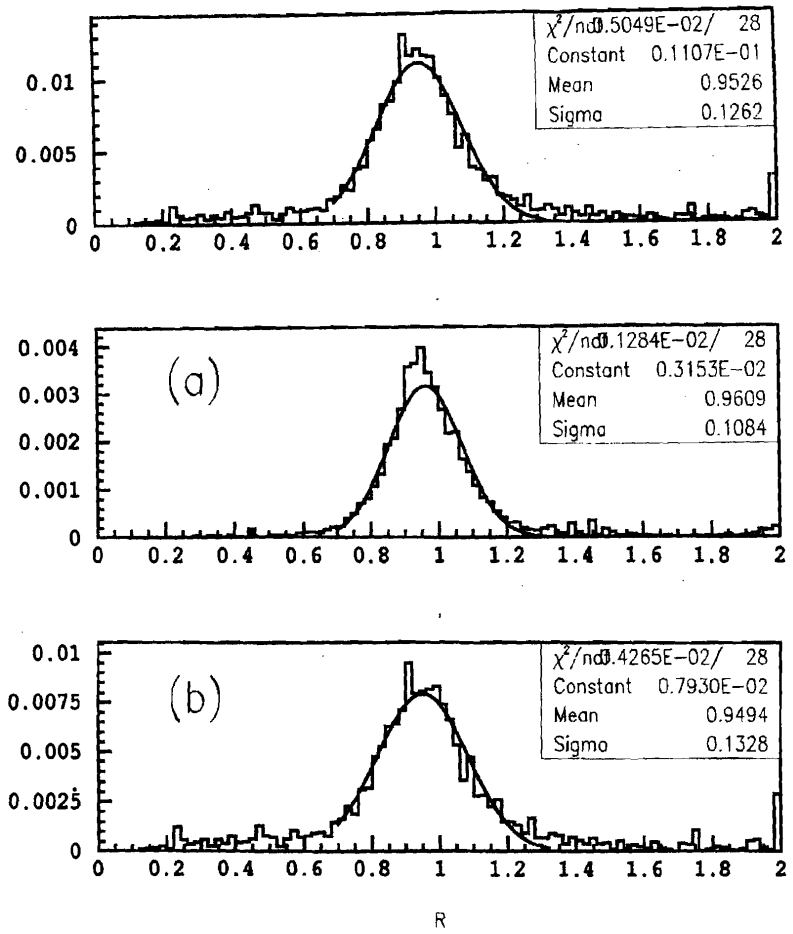

Figure 5. The ratio between the fitted and true momenta of the electron from $\tau^- \to e^-\nu\bar{\nu}$, $R = p_e^{\rm meas}/p_e^{\rm true}$, for all values of p_e (a), for $p_e < 5$ GeV (b), and for $p_e > 5$ GeV (c).

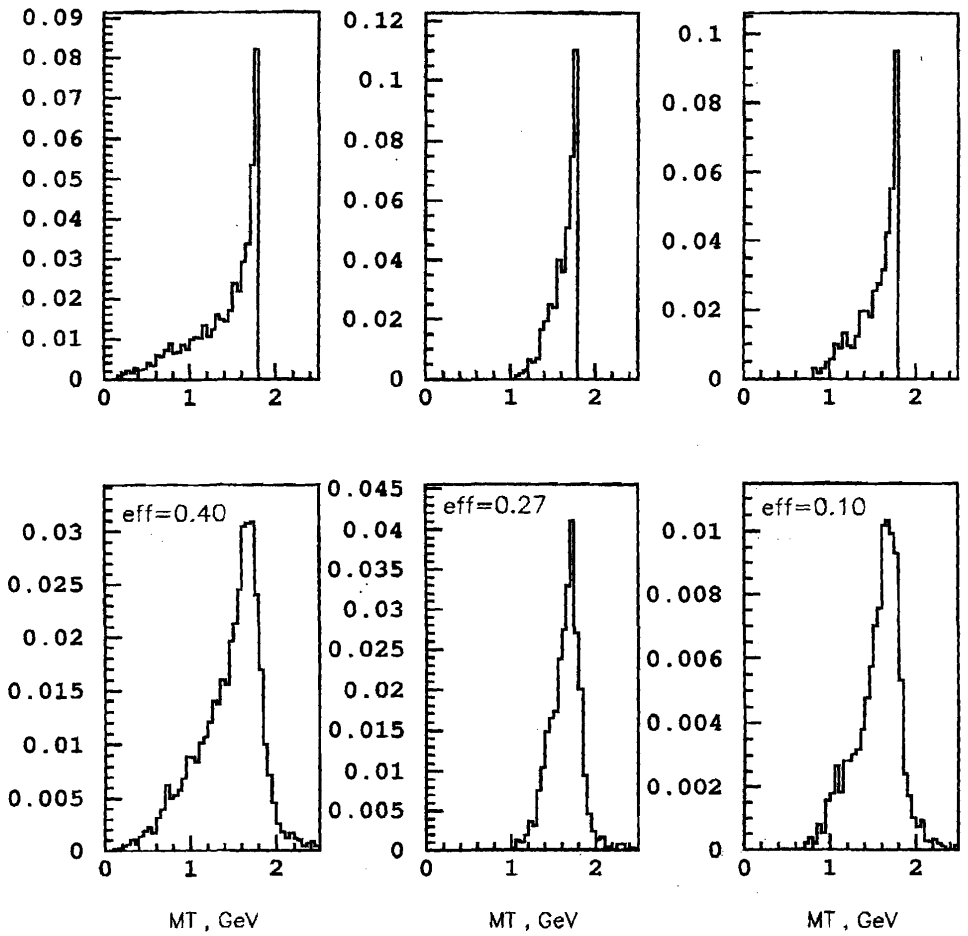

Figure 6. Transverse mass $M_{\rm T} = \sqrt{m_h^2 + p_{\rm T}^2} + p_{\rm T}$ for the (quasi-)two-body decays $\tau^- \to h^-\nu$ with $h^- = \pi^-$ (left-hand column), $h^- = \rho^- \to \pi^-\pi^0$ (middle column), and $h^- = a_1^- \to \pi^-\pi^+\pi^-$ (right-hand column). The unsmeared $M_{\rm T}$ distributions for all events in each channel prior to any selections are shown in the top row. The smeared distributions for detected events are shown in the bottom row.

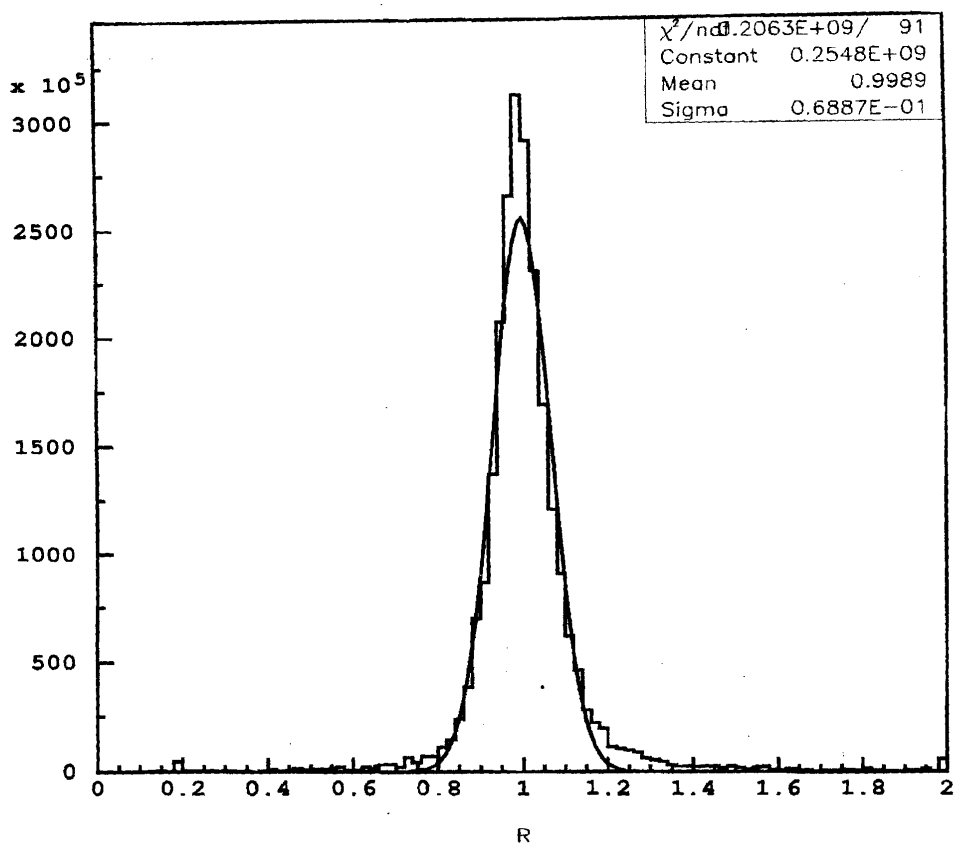

Figure 7. The ratio between the measured and true momenta, $R = p_\pi^{\rm meas}/p_\pi^{\rm true}$, for the π^- from the decay $\tau^- \to \pi^-\nu$.

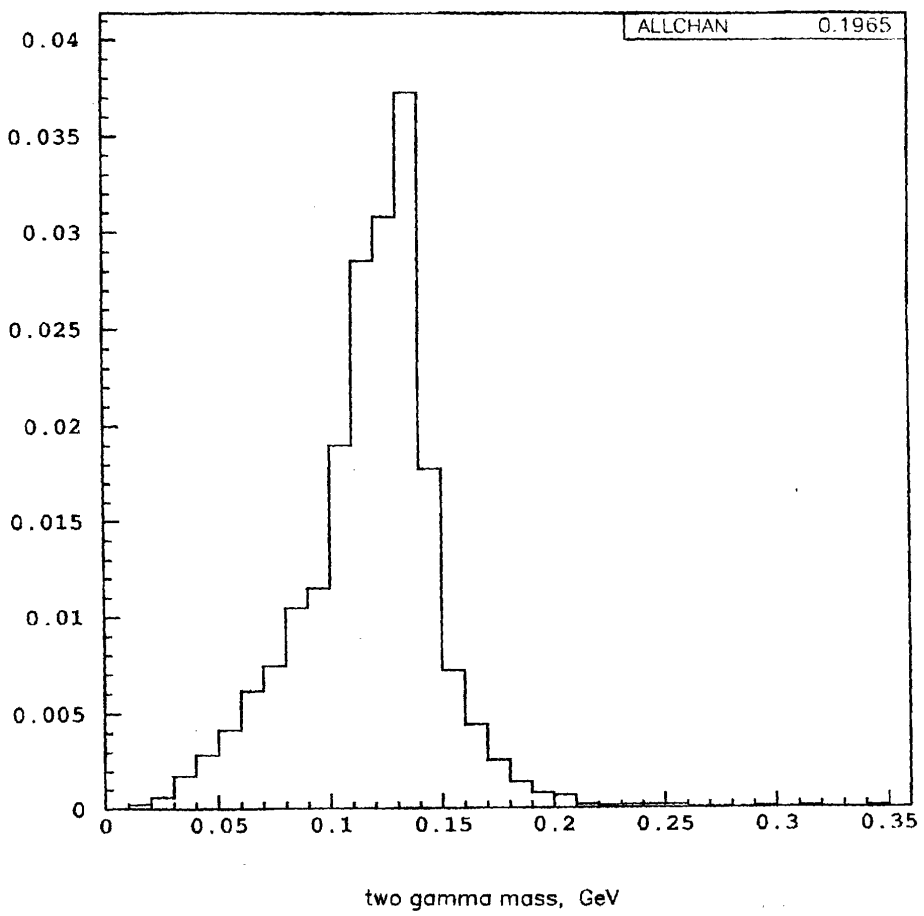

Figure 8. For the decay $\tau^- \to \pi^-\pi^0\nu$ followed by $\pi^0 \to \gamma\gamma$, the measured invariant mass of the two photons that have been detected either in the target or in the electromagnetic calorimeter.

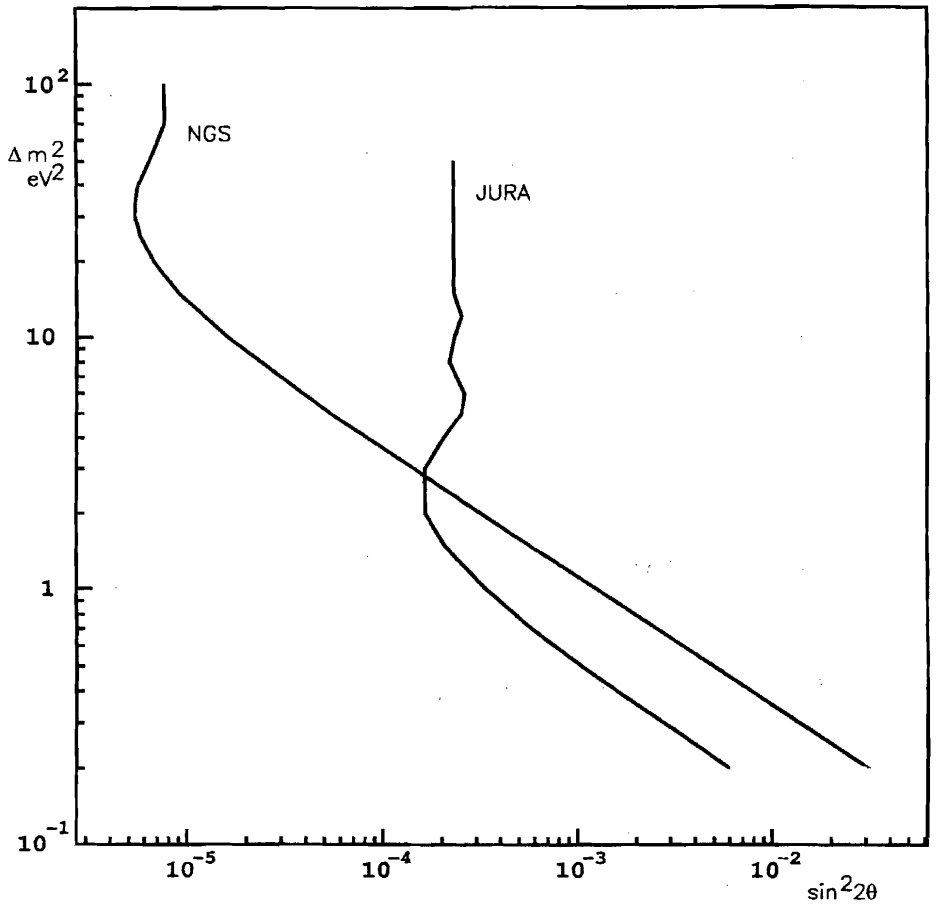

Figure 9. The null-limit exclusion plots (at 90% C.L.) for the medium-baseline experiment on Jura and for the short-baseline experiment on the near site of the NGS beam, assuming 10^{20} protons on target delivered by CERN-SPS.

References

[1] C. Athanassopoulos *et al.*, LSND Coll., Phys. Rev. Lett. 77, 3082 (1996).

[2] B. Achkar *et al.*, Nucl. Phys. B434, 503 (1995).

[3] L. Borodovsky *et al.*, E776 Coll., Phys. Rev. Lett. 68, 274 (1992).

[4] M.C. Gonzales-Garcia, H. Nunokawa, O.L.G. Peres, T. Stanev, and J.W.F. Valle, *Update on Atmospheric Neutrinos*, Phys. Rev. D58, 033004 (1998).

[5] F. Dydak *et al.*, CDHS Coll., Phys. Lett. B134, 281 (1984).

[6] N. Ushida *et al.*, E531 Coll., Phys. Rev. Lett. 57, 2897 (1986).

[7] ICARUS-CERN-Milano Coll., CERN/SPSLC 96-58, SPSLC/P304 (1996).

[8] E. Eskut *et al.*, CHORUS Coll., Nucl. Instr. and Meth. A401, 7 (1997); Phys. Lett. B424, 202 (1998).

[9] A. Ereditato, K. Niwa, and P. Strolin, INFN/AE-97/06, Nagoya DAPNU-97-07 (1997); H. Shibuya *et al.*, LNGS-LOI 8/97 (1997); K. Kodama *et al.*, CERN/SPSC 98-25, SPSC/M612 (1998).

[10] J. Altegoer *et al.*, NOMAD Coll., Nucl. Instr. and Meth. A404, 96 (1998).

[11] G. Acquistapace *et al.*, *The CERN neutrino beam to Gran Sasso*, CERN 98-02, INFN/AE–98/05 (1998).

[12] A.S. Ayan *et al.*, TOSCA Coll., Letter of Intent, CERN-SPSC/97-5, SPSC/I213 (1997).

[13] T. Nakano, Ph.D. Thesis, University of Nagoya (1997); G. Rosa *et al.*, Univ. Salerno DSF US 97/1 (1997), submitted to Nucl. Instr. and Meth.

[14] Eduardo do Couto e Silva, *Silicon Detectors for Neutrino Oscillation Experiments*, CERN-EP/98-081 (1998).

[15] K. Kodama *et al.*, E653 Coll., DPNU-96-33 (1996).

[16] K. Kodama *et al.*, COSMOS Coll., *Update Report on Fermilab E803/COSMOS* (1995).

[17] J.P. Revol *et al.*, *A Search Program for Explicit Neutrino Oscillations at Long and Medium Baselines with ICARUS Detectors*, ICARUS-TM-97/01 (1997).